Comparison of fluorescence of sodium fluorescein in retinal angiography with measurements *in vitro*

J. Ossewaarde-Van Norel
P. R. van den Biesen
J. van de Kraats
T. T. J. M. Berendschot
University Medical Center Utrecht
Department of Ophthalmology, E03.136
P.O. Box 85500
3508 GA Utrecht, The Netherlands

D. van Norren
University Medical Center Utrecht
Department of Ophthalmology, E03.136
P.O. Box 85500
3508 GA Utrecht, The Netherlands
and
TNO Human Factors
P.O. Box 23
3769 ZG Soesterberg, The Netherlands

Abstract. To quantify dye leakage in ocular fluorescein angiography, the arterial concentration of sodium fluorescein has to be determined. We investigated whether the nonlinear relationship between the fluorescein concentration and the fluorescence intensity obtained by *in vitro* measurements corresponds with that measured *in vivo* in a retinal artery. The time series of fluorescence in a retinal artery were recorded using an in-house-designed and -built confocal scanning laser ophthalmoscope in 11 healthy volunteers. Three different doses of sodium fluorescein were injected successively. About 10 min after the last injection a venous blood sample was drawn. The three *in vivo* peak intensities were fitted by least squares on the *in vitro* calibration curve using the first peak concentration and an intensity scaling factor as the two unknown parameters. The fit showed that the saturation of the three *in vivo* peak intensities corresponded well with the *in vitro* data. Calculation of the intensity scaling factor from the blood sampling data confirmed the result of the fit. The fitted concentration was verified by showing that the cardiac output necessary to obtain this concentration was within the physiological range. The fluorescence measured in our *in vitro* experimental setup corresponded well with the *in vivo* measurements. Therefore, the results from *in vitro* measurements can be applied in the analysis of fluorescein angiograms. © *2002 Society of Photo-Optical Instrumentation Engineers.* [DOI: 10.1117/1.1462034]

1 Introduction

In ophthalmology, sodium fluorescein is used to visualize pathology of the retina and the choroid. After intravenous injection, the bolus passage in the ocular fundus is documented by taking pictures for several minutes. An increase in fluorescence after passage of the first dye indicates abnormal dye leakage into the extravascular space in that area. In clinical practice, the evaluation of dye leakage is qualitative and subjective. Using quantification, objective criteria for the classification of diseases and the evaluation of therapies might be designed.

Since dye leakage depends on the intravascular dye concentration, the dye concentration in the ocular vessels must be known in order to quantify extravasation. To convert the time series of intravascular fluorescence intensities into concentrations, an *in vitro* calibration curve and a scaling factor between intensities *in vitro* and *in vivo* are required. The relationship between the concentration and fluorescence in blood has been determined *in vitro*.[1–4] It was shown to be nonlinear: with an increase in concentration, the concentration–intensity curve (*CI* curve) levels off and even decreases at higher concentrations, although the latter condition is not met in clinical doses. The two most important reasons for this nonlinear behavior are self-absorption and quenching. First, in frontal illumination and detection (used in fluorescein angiography), absorption of excitation and emission light by blood and fluorescein in superficial layers causes the contribution of deeper layers to the fluorescence to decrease to zero. This self-screening results in a leveling off of the *CI* curve with an increase in layer thickness. In blood almost all fluorescence originates from the superficial 50 μm.[2,4] Scattering of light by the red blood cells appears to have only a minor beneficial effect on fluorescence.[2] The second phenomenon is collisional or dynamic quenching, which leads to reduced quantum efficiency of the fluorescence process due to an increase of collisions between excited fluorescein molecules or with other (solvent) molecules at higher concentrations. Furthermore, at higher concentrations, polymerization or static quenching can occur due to the formation of nonfluorescent dimers and polymers, which absorb, but do not emit light.[5] Many physicochemical factors influence the shape of the concentration–intensity curve,[6] for example, the oxygen saturation of the blood,[2] the pH,[1,6] the aggregation level of red blood cells,[4] the fraction of free fluorescein (because its fluorescence efficiency is about 2.2 times that of bound fluorescein[7]) and the presence of quenchers.[6] Because several of these factors may act differently *in vitro* and *in vivo*, it is not clear whether the *CI* curve is similar under both conditions. In addition, fluo-

Address all correspondence to J. Ossewaarde–Van Norel. Tel: +31 30 2507907; Fax: +31 30 2505417; E-mail: a.vannorel@oogh.azu.nl
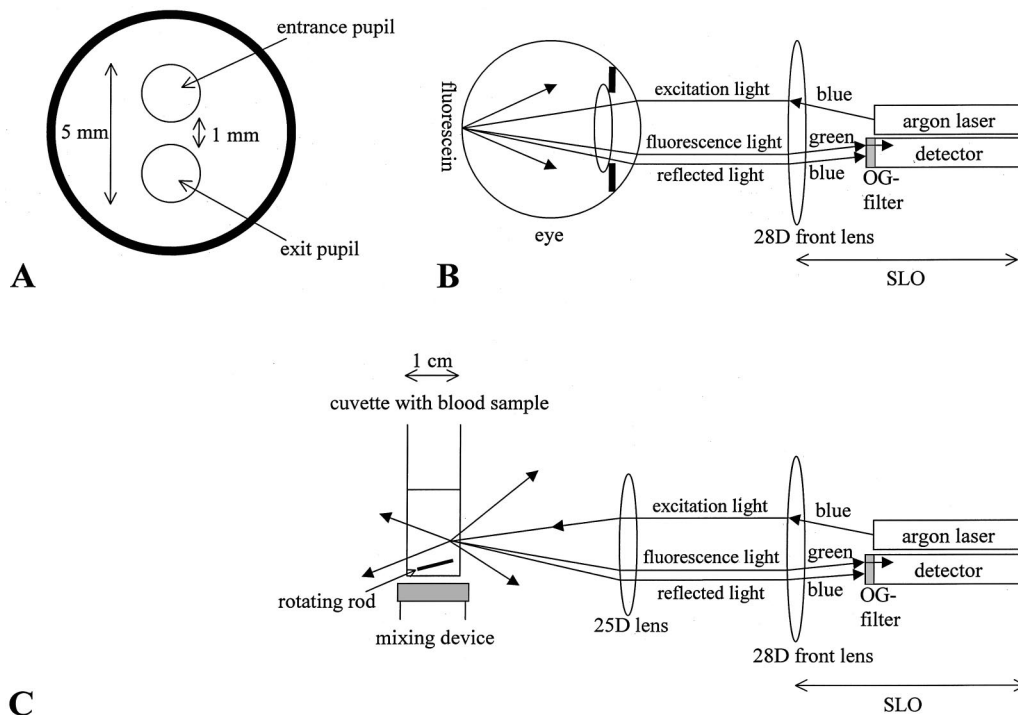
Fig. 1 Pupil configuration of the SLO designed to reduce ocular stray light: frontal (A) and sagittal views (B). Optical arrangement for *in vitro* measurements; the 25 Diopter lens and the cuvette have replaced the eye (*C*).

rescence measurements in blood artificially kept in motion in a cuvette may differ from that in a retinal artery, due to the (unknown) influence of the vessel wall and flow characteristics on fluorescence.

The purpose of this paper is to describe an experimental setup to measure fluorescence intensities in blood *in vitro* and *in vivo* in retinal arteries and to investigate the relation between them.

2 Materials and Methods

2.1 Study Design

In blood, fluorescence intensity was measured *in vitro* as well as *in vivo* as a function of the fluorescein concentration. The *CI* curve *in vitro* was obtained by measuring the fluorescence intensities (in arbitrary units) of several known sodium fluorescein concentrations in sampled blood. *In vivo*, the actual concentration in the retinal arteries was unknown. However, by using three different injection doses with a fixed ratio of 1:10:20, the ratio of the peak concentrations in the retinal arteries was known (1:10:20). Due to the difference in optics, the three peak intensities measured *in vivo* differed from the intensities measured *in vitro* by an unknown scaling factor. On a $\log I$ vs $\log C$ scale, the graph of the *in vivo* points was shifted horizontally and vertically until the *in vivo* points coincided with the *in vitro* calibration curve as well as possible, i.e., by minimizing χ^2. The *in vivo* concentration values and the intensity scaling factor were derived from the horizontal and vertical shifts, respectively. The values obtained were verified by an independent experiment and two calculations.

2.2 Instrument

For fluorescein angiography and for the *in vitro* measurements we used an in-house-designed and -built confocal scanning laser ophthalmoscope (SLO). In contrast with an earlier version of this instrument,[8] an aspherical front lens of 28 Diopters was used to obtain a larger field of view ($40° \times 23°$). The position of the lens could also be adjusted to correct ametropia. A special feature of this SLO was the absence of an overlap of outgoing and incoming light, thus reducing stray light. Figure 1 shows the pupil configuration [Figure 1(A)] and a schematic of the in- and outgoing beams [Figure 1(B)].

For excitation of the fluorescein an argon laser beam of 488 nm was used, which scanned a retinal area of $40° \times 23°$ (refresh rate of 50 Hz). By means of a confocal retinal aperture in the optics of the SLO, a retinal detection area of 1.35° centered around this laser spot, scanning the retinal area concurrently, was defined to reduce the level of stray light. The diameter of this retinal detection area was much larger than the diameter of the focus of the laser beam (0.06°) to ensure that the detection area fully covered the illumination area even when their centers did not coincide due to residual refractive errors. Before reaching the photomultiplier tube, the returning, descanned light from the fundus passed an OG515 high pass filter to select the green fluorescent light and to block reflected excitation light. The intensity of the output video signal is proportional to the amount of fluorescence light detected by the photomultiplier. The video amplifier was DC coupled to avoid dynamically induced changes in the level.

During image acquisition there were 488 nm flashes (40 ms) at a maximum rate of 0.9 Hz. In between these flashes

only a 635 nm red cross was shown for eye fixation.

Retinal exposure limits for thermal and blue-light photochemical retinal hazards were calculated using the revised guidelines of the International Commission on Non-Ionizing Radiation Protection.[9] The power of the 488 nm laser beam was 2.1 mW in front of the front lens. Even in the case of breakdown of the scanner, the exposure limit for thermal damage was three orders of magnitude higher than exposure from our laser. Considering the exposure limits for photochemical damage, the retinal irradiance of 2.69 mW/cm^2 allowed a safe exposure time of over half an hour, much longer than the total exposure time per subject (25 s at most).

A bite board with a dental compound and two forehead rests ensured proper fixation of the subject's head.

Following each angiogram, a blue reflection image of a plate covered with white reflectance paint (Eastman Kodak Company$^®$) was obtained for calibration of the laser intensity and for the off-line correction of the slight inhomogeneity of the fundus' illumination (a gradual drop in intensity towards the borders of the image). This white reflectance paint had near unity diffuse reflection of light in a broad spectral range. The correction required for the inhomogeneous fundus illumination was mainly in the horizontal direction. Thirty pixels from the left border of the image and 20 pixels from the right border the pixel intensity was 50% of the maximum (correction factor=2). The area of analysis was always located more centrally in the image.

2.3 Image Processing

Off-line analysis of the recorded images of 512×512 pixels consisted of several steps. Firstly, the inhomogeneity of the fundus illumination was corrected using the image obtained from the white plate described above. After this image was corrected for being plane instead of concave, and smoothed to remove small structural details in the paint layer, all angiographic images were divided by this image. Second, the minor translational and rotational eye movements during image acquisition were compensated for by translating and rotating each image until two designated vessel crossings coincided with those in a bright reference image taken near the arterial bolus peak. Images taken during major eye movement were rejected. Third, the pixel gray values were corrected for the variation in gain levels during the angiogram. Finally, a straight segment of a retinal artery with a diameter of at least 50 μm was selected to obtain the arterial time–intensity curves. Sixteen adjacent line profiles were selected perpendicular to the vessel axis. Their mean intensity profile was displayed on the monitor. From that, the pixel value in the vessel's center was designated to constitute one point of the arterial time–intensity curve.

2.4 Participants

Eleven healthy volunteers (2 males and 9 females, age 19–26 years, mean age 21.8 years) underwent fluorescein angiography. The Medical Ethical Committee of the University Medical Center Utrecht approved the procedures that were in accordance with the Declaration of Helsinki. Written informed consent was obtained from each volunteer after an explanation of the procedure. None of the subjects had ophthalmic or cardiovascular complaints, nor contraindications against fluo-
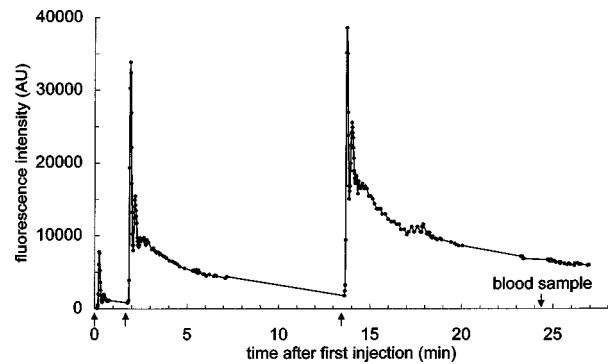
Fig. 2 Time course of the fluorescence intensity measured in a large retinal artery with three subsequent intravenous injections of fluorescein (subject No. 6). The line connects the data points. The arrows beneath the vertical axis indicate the times of injection.

rescein injection. Their pupils were dilated with two drops of 0.5% tropicamide and two drops of 5% phenylephrine. A cannula (Vasculon, 20 gauge) was inserted into the antecubital vein; 20 mL blood was drawn into ethylene-diamine-tetraacetic-acid (EDTA)-filled tubes. The waist of the SLO scan was adjusted in the upper part of the pupil's plane in such a way that at least 1 mm separated both the entrance and exit pupil from the border of the iris [Figure 1(A)]. The fundus image was optimized for sharpness and vignetting on a television monitor by adjusting the position of the front lens. Patients were instructed to maintain eye fixation and a stable head position during the angiography.

2.5 In Vivo Measurements

Three quantities of fluorescein were injected: first 18 mg/m^2 body surface,[10] after about 100 s followed by 180 mg/m^2 body surface. Approximately 11 min after the first injection a final injection of 360 mg/m^2 body surface was given (Figure 2 depicts the three intra-arterial fluorescence peaks resulting from these three injections). To achieve the same bolus shape the volumes injected were kept constant: the highest dose was prepared using the 20% fluorescein solution. The lower doses were prepared by diluting 20% fluorescein solution in 5% glucose to obtain the same volume as the volume of the third bolus.

To obtain reproducible compact bolus profiles, a standardized means of injection was essential. In earlier angiograms we obtained severely disturbed inflow curves resulting from fluorescein that was retained in the arm after injection.[11] To avoid such irregularities we standardized the procedures. The fluorescein was injected as fast as possible (within 1 s) to obtain a compact and reproducible bolus configuration. All injections were given by the same experimenter. The injections were followed by a 10 mL flush of 5% glucose. The bolus profile was further improved by (1) warming the arm with an infrared lamp prior to the injections to improve circulation in the arm, (2) applying a tourniquet just distal to the injection site to prevent retrograde flow of fluorescein towards the hand during injection, and (3) asking the subject to make a fist 15 times immediately after the injection and release of the tourniquet to enhance circulation in the hand and thus the venous flow. Several minutes after the second and third injections all subjects were asked to move their arm up- and down-

ward to check that no additional inflow of fluorescein occurred several seconds later due to residual fluorescein in the arm.

Image acquisition started 7 s after the injection of the first bolus and continued for about 25 min, interrupted by two breaks about 5 min after both the second and the third injections. During the first bolus passage the image acquisition rate was set to maximum (one image per 1.1 s).

2.6 *In Vitro* Measurements

Immediately after fluorescein angiography the venous blood samples were oxygenated by air exposure to achieve (arterial-like) oxygen saturation levels of at least 90%: the blood was gently shaken in wide containers to enlarge the contact surface between the blood and air. Measurements showed that the oxygen saturation of the blood after this procedure was at least 90%. For calibration purposes, sodium fluorescein concentrations of 0.02, 0.06, 0.10, 0.20, 0.30, 0.50 and 1.0 mg/mL were prepared in 1 mL autologous blood collected prior to the injection of fluorescein. The required fluorescein solutions had been prepared by diluting 20% fluorescein in phosphate buffer (pH 7.38). By using autologous blood to obtain a calibration curve the same hemoglobin concentration as that in the eye was ensured. The dilution factor by adding fluorescein (20 μL) to the blood (1000 μL) was not significant.

The fluorescence intensities of the blood samples were measured in an experimental setup, shown in Figure 1(C). A 25 Diopter lens was used to focus the laser beam onto the surface of the blood in a 10 mm sq cuvette. This lens was placed in the waist of the scan beam, similar to in the human pupil plane. Measurements in a 10 mm thick blood layer *in vitro* will result in similar intensities to those that would have been measured in a layer of the same thickness as a large retinal artery (about 100 μm), since 90% of the total fluorescence originates from the superficial 50 μm of the blood column.[2] The blood sample was kept in motion by a rod that rotated at the bottom of the cuvette to prevent aggregation of the red blood cells and the formation of plasma gaps between the aggregates that might allow a contribution from deeper layers, resulting in higher fluorescence intensities.[4] The value of the background pixel (mainly an electronic offset and only a small amount of stray light) measured in the blood sample that contained no fluorescein was subtracted from all the intensities measured. All concentrations were prepared and measured in duplicate at room temperature, within a few hours after the vein was punctured. For each concentration, the four measured intensities were averaged. Previous experiments had shown that the fluorescence intensities in blood samples remained constant for at least 2.5 h.

2.7 Analysis

We have used an ad hoc function to describe the relation between the log dye concentration and log fluorescence intensity within the physiological range of concentrations (below the peak of the curve of about 1–2 mg/mL)[2,4] and at the beginning of the descending part of the curve observed in the *in vitro* experiments (Appendix A).

To compare the *in vivo* data with the *in vitro* data we used a fit procedure. First, the fit was performed on the data sets of

each subject separately. The three peak intensities measured *in vivo* had to be scaled by a factor to be determined by the fit procedure to the intensities obtained in the *in vitro* curve (Figure 3, open symbols). In addition, the concentrations during the angiogram were unknown. However, the ratios between the peak concentrations were known and could be used in the fit: the strict injection protocol assured that the shape of the three peaks was similar, with an amplitude ratio of 1:10:20. When using the ratio of the three peak intensities, the residual fluorescence values prior to injection of the second and the third bolus had to be taken into account: the residual fluorescence intensities were converted into concentration values using the function given in Appendix A, and then subtracted from the peak concentrations. Thus, on a logarithmic scale the three *in vivo* data points had to be shifted both vertically and horizontally to fit the *in vitro* data. This fit was optimized by minimizing χ^2, in which the standard deviation was considered to be equal for all data points (Figure 3).[12]

After transformation to a linear scale, the fit yielded both the first peak concentration and an intensity scaling factor (k_{fit}):

$$k_{\text{fit}} = I_{in\ vitro}/I_{in\ vivo}. \qquad (1)$$

For a fit performed on a data set of one subject, the 68% confidence intervals for the intensity scaling factor (k_{fit}) and the first peak concentration could not be calculated, because the measurement errors of the *in vivo* data points were unknown. Therefore, the fit was also performed on the mean of the logarithms of the data of all subjects. Since we cannot discriminate between measurement errors and biological variation as a cause of variation in the shape of the *CI* curves, all sources of variation were combined and estimated by the standard error of the mean. However, the value was influenced by the absolute level of the individual data, which was determined by the amount of light absorption in the ocular media, the length of the eye axis, etc. To compensate for differences in the absolute levels of the data sets, each log data set was shifted vertically until its mean coincided with the mean of the three log peak intensities of all subjects (normalization). Next, the standard errors of the mean of these normalized log peak intensities were calculated and used in the fit and the calculation of the 68% confidence intervals of the fitted parameters (Figure 4). Similarly, this normalization was also performed on the *in vitro* curves to calculate the standard errors of the mean for each data point.

2.8 Verification of the Fitted Results

The fit yielded both the first peak concentration and an intensity scaling factor (k_{fit}). The plausibility of the values was verified in three ways: (1) calculation of the cardiac output from the first peak concentration, (2) blood sampling after the third fluorescein injection to measure the intensity scaling factor ($k_{\text{blood sample}}$) and (3) optical calculation of the intensity scaling factor (k_{optical}).

(1) The peak concentrations should be the result of physiological cardiac output. Cardiac output (CO) (L/min) is equivalent to

$$CO = A \bigg/ \int_0^{te} C(t)dt, \qquad (2)$$
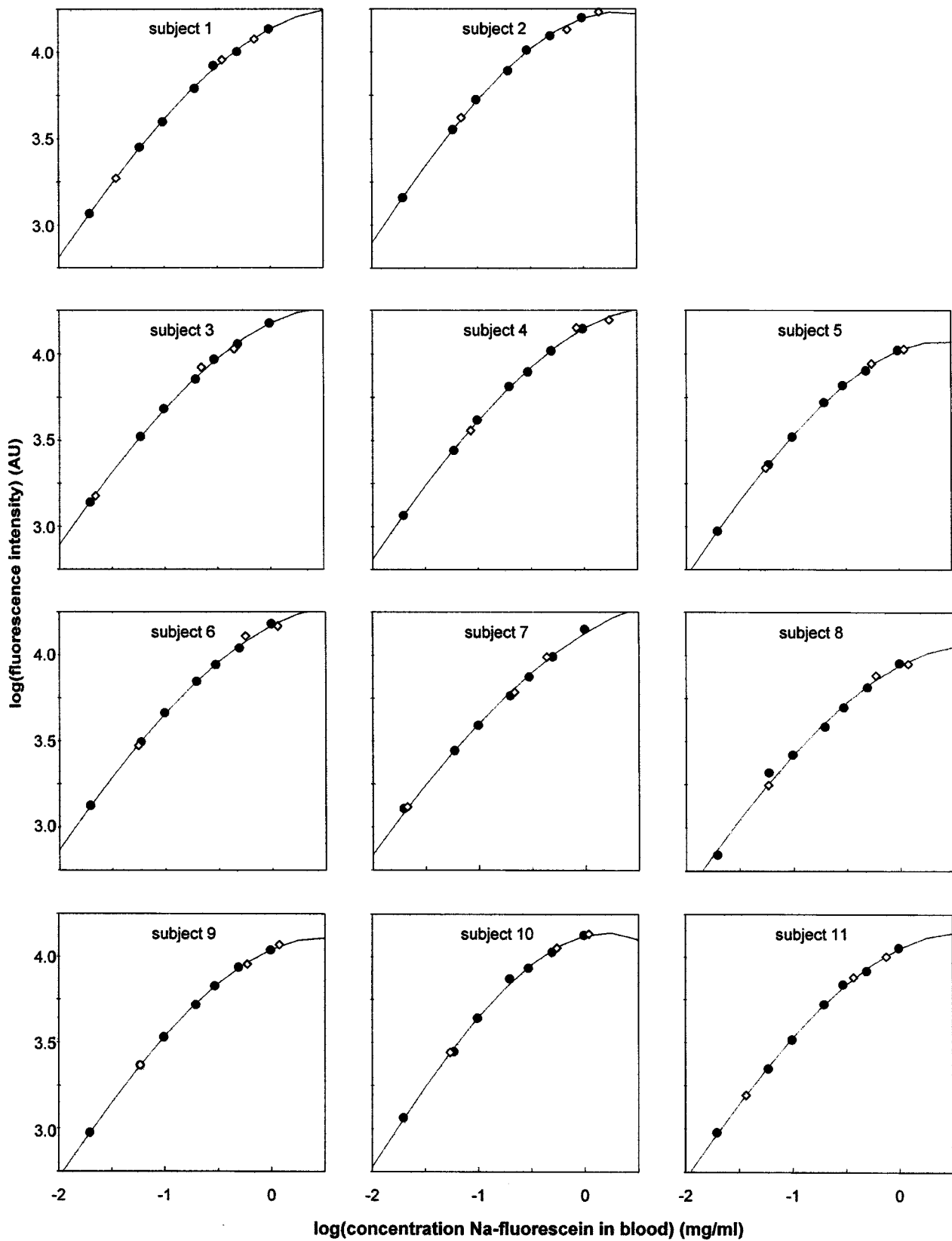
Fig. 3 Concentration–intensity curves; comparison between *in vitro* (●) and *in vivo* (◇) data in 11 subjects. The *in vitro* data points were fitted by the function given in Appendix A (smooth line). The *in vivo* data points were matched to the *in vitro* curve by minimizing χ^2. Both the fluorescence intensities measured *in vitro* and *in vivo* are expressed in the same units (AU=arbitrary units=pixel gray values corrected for the gain), but $\log(k_{fit})$ was added to the *in vivo* intensities (see the note at the top of Table 1).
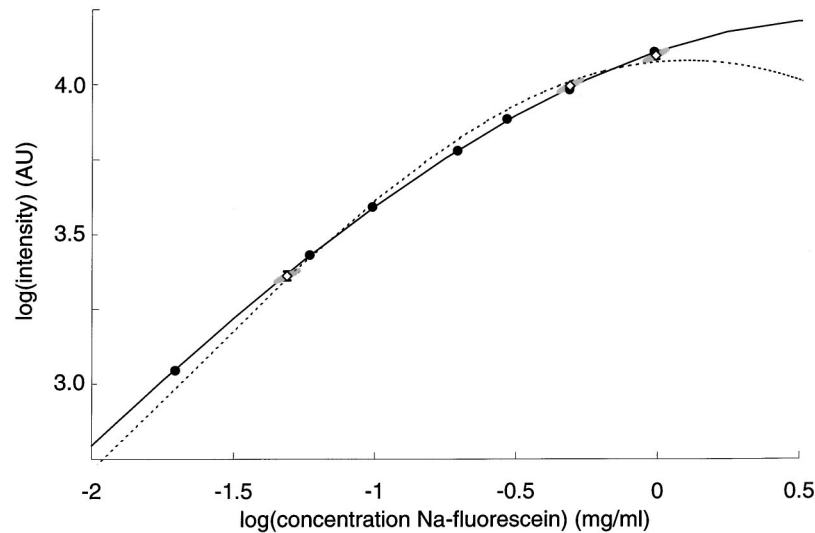
Fig. 4 Mean concentration–intensity curve measured *in vitro* (●), fitted by the function given in Appendix A (smooth line) together with the mean *in vivo* data points that were fitted (◇). Vertical error bars represent the standard error of the mean, but especially in case of the *in vitro* data, these are too small to be visible. The ellipses represent the 68% confidence two-dimensional intervals. The broken line shows the result of the fit of the physiological description of the saturation of the *CI* curve to the data (see Appendix A).

where *A* is the amount of dye injected (g) and *te* the time (min) at which the dye concentrations (g/L) have returned to zero. Using a typical bolus profile after the first injection, the data points at the beginning of the inflow curve up to those that are two third of the peak value in the downslope phase, thus excluding the recirculation phase, were fitted with a gamma function to derive *te*. Next, the cardiac output was calculated.

(2) To check the intensity scaling factor obtained from the fit (k_{fit}), this factor was also obtained from an oxygenated blood sample that was drawn between 10 and 13 min after injection of the third bolus from the contralateral antecubital vein in an EDTA-filled tube ($k_{blood\ sample}$). In a pilot experiment (three angiograms) we have verified that at this time of blood sampling the mixing of fluorescein over the body has been completed by drawing and measuring multiple blood samples between 4 and 26 min after the third injection. This is in agreement with the conclusion of Lund-Andersen et al.,[13] who estimated that the net extraction of fluorescein in peripheral capillaries is minimal 4 min after injection.

At least five fundus images were taken immediately before and after this blood sampling. To calculate the *in vivo* intensity at the time of blood sampling ($I_{in\ vivo}$) the data points before and after blood sampling were interpolated by fitting the decay curve with an exponential function. The intensity scaling factor *k* was

$$k_{blood\ sample} = I_{in\ vitro}/I_{in\ vivo}. \qquad (3)$$

(3) The intensity scaling factor was also calculated on the basis of comparing *in vivo* and *in vitro* optical pathways ($k_{optical}$). These calculations are summarized in Appendix B.

3 Results

3.1 *In Vivo* Measurements

A typical example of a time–intensity curve is shown in Fig. 2. Three main peaks are visible as a result of the three injections of fluorescein. Due to the shape of the compact bolus, recirculation of the bolus is visible as a small peak about 15 s after the main peak. The effect of quenching and self-absorption can be observed in the peak intensities: the third peak is only slightly higher than the second peak, although the dose injected was twice as high as that in the second injection.

3.2 *In Vitro* Measurements and Analysis

The concentration–intensity curves determined *in vitro* in all 11 subjects are depicted in Fig. 3 (closed symbols). Also in Figure 3 the three *in vivo* data points are plotted (open symbols): the three fitted log peak concentrations constitute the *x* values. The *y* values of the three *in vivo* data points (intensities that are comparable with the *in vitro* intensities) are derived by summation of the log fitted intensity scaling factor [$\log(k_{fit})$] and the log intensities measured in the retinal artery. Figure 4 displays the mean results. In Figure 4 the vertical error bars show the standard errors of the mean. The error bars of most of the data points are smaller than the symbols. The 68% confidence intervals of the first peak concentration and the intensity scaling factor (k_{fit}) were determined by calculating ($\chi^2_{min}+1$) contours.[12] The confidence interval of the intensity scaling factor (k_{fit}) was converted into intensity values. The two-dimensional confidence intervals of the *in vivo* data points are shown as ellipses surrounding the data points (Figure 4). The *in vivo* data points could be brought to an accurate match with the *in vitro* curve. The rather small confidence intervals of the fitted parameters (the first peak concentration and the intensity scaling factor, Figure 4) ensure that estimation of the parameters is satisfactory.

Table 1 First peak intensities measured, peak concentrations according to the fit and intensity scaling factors according to the fit and the blood sampling data after the third injection. Note: To derive the y values in Figure 3, the [log first peak intensity + log k(fit)] should be calculated.

Subject No.	First peak intensity (a.u.)	First peak concentration (mg/mL)	k_{fit}	$k_{blood\ sample}$	Relative deviation of k_{fit} from $k_{blood\ sample}$ (%)
1	2802	0.035	0.664	0.679	−2
2	11804	0.071	0.355	0.362	−2
3	4398	0.022	0.343	0.443	−23
4	8642	0.085	0.419	0.364	15
5	3777	0.055	0.581	0.631	8
6	7772	0.056	0.381	0.433	12
7	4579	0.021	0.285	0.394	28
8	5375	0.058	0.328	0.277	18
9	5484	0.059	0.425	0.423	0
10	7912	0.054	0.350	0.368	5
11	3541	0.037	0.442	0.464	5
Fit on mean	5567	0.049±0.005	0.41±0.03	0.44±0.12	−6

The peak intensities of the first bolus are listed in the second column of Table 1, and the peak concentrations following the first injection derived from the fit in the third column. The mean dose given was 33.3 mg (a range of 30.1–37.8 mg), resulting in a mean peak concentration of 0.049 mg/mL [±0.005 standard deviation (SD)]. The intensity scaling factors that result from the fit are listed in the fourth column of Table 1. The mean is 0.41±0.03.

3.3 Verification of the Fitted Results

To verify the peak concentrations obtained from the fit, the cardiac output was calculated. According to Eq. (2), using the mean value of the dose and the first peak concentration, the mean cardiac output would be about 7.6 L/min. This value is within the physiological range.[14]

The intensity scaling factor according to the fit (k_{fit}) was compared with the results of the two other methods. The intensity scaling factors resulting from the blood samples after the third injection ($k_{blood\ sample}$) are shown in the fifth column, the mean $k_{blood\ sample}$ was 0.44±0.12. Furthermore, from the optical calculations an intensity scaling factor ($k_{optical}$) of about 0.54 was derived (Appendix B). These three independent determinations of k yield values (0.41±0.03, 0.44 ±0.12, and 0.54±0.14) that are not significantly different.

4 Discussion

The saturation of the three *in vivo* peak intensities corresponded well to the *in vitro* data (Figure 4). However, a satisfying fit does not imply that the *in vivo* results are realistic. To check whether the concentrations and the intensity scaling factor were plausible, these results were validated by other data and calculations. First the mean estimated cardiac output

was about 7.6 L/min (normal value at rest: 5–5.5 L/min). Anxiety, not improbable in this experiment, could increase the cardiac output by 50%–100%.[14] Therefore, the first peak concentration (and thus also the second and third) was physiologically plausible.

In addition, the intensity scaling factor obtained from the fit (k_{fit}=0.41±0.03) was in good agreement with the intensity scaling factor derived from the blood samples drawn after the third injection ($k_{blood\ sample}$=0.44±0.12) and with the calculations on the basis of the *in vivo* and *in vitro* optical pathways ($k_{optical}$=0.54±0.14).

From these results we conclude that the leveling off of fluorescence intensities at higher dye concentrations measured under *in vitro* conditions follows the same pattern as that in retinal arteries. Apparently all physicochemical variables that are able to significantly influence the shape of the *CI* curve (see Sec. 1) did not differ between the *in vivo* and the *in vitro* measurements. Unknown variables that influence the shape of the *CI* curve also play a role in our *in vitro* measurements, as can be concluded from the mismatch between a physiological mathematical description of the *CI* curve (based on self-absorption and quenching; see Appendix A) and our data. The reliable results from the fit showed, however, that these unknown (and uncontrolled) variables did not differ much from the *in vivo* circumstances or that their net effect was not substantial. The *in vitro* and the *in vivo* data sufficiently corresponded with each other for the main purpose of quantifying the amount of dye leakage during angiography.

Inevitably, the *in vivo* measurements have some sources of error. A proper injection technique is essential for this type of study. All fluorescein injected should pass the retinal circulation as one bolus. Only in subject No. 7 did a minor additional

peak occur due to movement of the arm after the third injection. Apparently, a small amount of fluorescein was retained in the arm, in spite of all the precautions. The curve of subject No. 2 showed a slight disturbance during the first recirculation after the second bolus without an apparent cause.

The amount of stray light (fluorescence from neighboring structures resulting from dispersion of the excitation light in the ocular media and possibly from the tissue layers in front of the blood vessels) measured *in vivo* was unknown. Although the entrance and exit beams of our SLO were separated, they coincided of course at the retinal level. As a result, low background fluorescence (fluorescence from areas adjacent to the vessel) could be measured when measuring in the center of a retinal vessel. By testing the SLO with black lines of varying widths on a white screen, we measured in the center of a black line, simulating a vessel of 150 μm, 3%–4% of the intensity of the white screen. However, we expected the level of stray light *in vivo* to be higher. Let us consider the worst case of a myopic fundus with relatively narrow retinal arteries and high background fluorescence. Based on measurements of the fluorescence intensities in a retinal artery on a dark background and on an adjacent light background in the early phase of the angiogram, we calculated the contribution of stray light to the intensity measured to be about 8%. If the peak intensities measured in the vessel's center were 8% too high due to stray light from the surrounding background, k_{fit} would be 8% too low. Considering the intensities in the retinal vessels, the relative magnitude of the background fluorescence increased during the angiogram (about 40% of the vessel's intensity during the first minute versus 49% 5–13 min after the third injection). Therefore, in this study $k_{blood\ sample}$ might have been underestimated by about 10%. If we had corrected for the stray light level *in vivo*, both k_{fit} and $k_{blood\ sample}$ would be closer to $k_{optical}$ ($k_{fit} = 0.44$ and $k_{blood\ sample} = 0.48$ versus $k_{optical} = 0.54$), thereby supporting our conclusions.

Another potential source of error was the diffusion of fluorescein into the vitreous. Such fluorescein could act as an absorber of excitation and fluorescence light. To study this as a source of error, we measured the intensities in the nonvascular zone of the fovea. In this area, macular pigment and melanin largely reduce the choroidal fluorescence and no retinal fluorescence exists. No slow rise of the fluorescence in this area was observed. Thus, at least in normal subjects the diffusion of fluorescein into the vitreous could be neglected.

In our *in vitro* experiments we attempted to control the main variables that influence fluorescence intensity. The hemoglobin concentration, pH, oxygen saturation and the optics and detector of the measurement device were similar *in vitro* and *in vivo*. The phenomenon that 90% of the fluorescence originates from the superficial 50 μm ensured that the effective thickness of the layer in which was measured *in vitro* was similar to the *in vivo* circumstances. By mixing the blood in the cuvette during measurement, another major prerequisite for fluorescence measurements, i.e., complete dispersion of erythrocytes in plasma, was achieved, but obviously the erythrocyte free zone near the vessel's wall was not achieved *in vitro*. Furthermore, for practical purposes, the *in vitro* measurements were done at room temperature instead of at body temperature. Third, blood was collected in EDTA-filled tubes to prevent blood clotting. EDTA prevents coagulation by

binding calcium, which is essential for the clotting process. It preserves the cellular components of blood. To our knowledge, no information is available in the literature on the influence of EDTA on the quenching behavior of fluorescein. According to our analysis these three factors (the erythrocyte-free zone, temperature, and anticoagulants) did not have a major influence on the fluorescence behavior of fluorescein *in vitro*.

In conclusion, we demonstrated that the *in vitro* fluorescence measurements in blood, described above, corresponded well with the *in vivo* measured fluorescence of fluorescein flowing through the ocular arteries. Using a calibration curve and an intensity scaling factor, the concentration curve in ocular arteries could be constructed from the intensities in the early phase of the angiogram. Since the leakage of dye depends on the intravascular dye concentrations, quantification of leakage becomes feasible.

Acknowledgments

Appendix A

Delori et al. proposed a physiological description of the saturation of the *CI* curve.[2] They assumed that quenching does not affect the rise of the *CI* curve and described this by the self-absorption of excitation and emission light in blood and fluorescein using Lambert–Beer law. To also allow quenching to cause part of the saturation of the curve, we added the Stern–Volmer equation[5] to the description of Delori et al. and fitted the function to the data by minimizing χ^2 (free parameters are the quenching constants, the quantum efficiency and the hematocrit). Figure 4 shows this physiological description of our data after the fit (broken line). Obviously, this description is not satisfactory. Without quenching (only self-absorption) the fit resulted in a hematocrit of 0.28, which is very unlikely. Assuming a higher hematocrit resulted in a fit that was poorer than the fit also taking quenching into account. We have no explanation for the different shape of our data compared to the physiological description and the data of others.[2] The main purpose of this study, however, was to check whether the *in vitro* curve resembles the *in vivo* curve. In the analysis we only need a simple way to interpolate between the *in vitro* data points.

Therefore, the *in vitro* data shown in Figures 3 and 4 were fitted with an invertible ad hoc function. We emphasize that the particular function used was merely a tool to deduce concentration values from intensity values and vice versa and does not have any physiological meaning.

$$\log I = a \sin[(b \log C + c)^6] - d,$$

with I being the fluorescence intensity, C the concentration, sin in radians and a, b, c, and d constants. The constants were obtained by a least square fit of the data points, on the condition of a slope of unity at low concentrations (arbitrarily chosen as 0.001 mg/mL). For Figure 4, e.g., $a = 11.55$, $b = 0.025$, $c = 1.06$, and $d = 7.34$. This function enabled the

conversion of fluorescence intensities measured *in vivo* to dye concentrations in the range of 0.000 01 (below the detection limit of the SLO) to 2 mg/mL.

Appendix B

Inevitably, differences in the optical setup exist between a measurement *in vivo* and one *in vitro* (Figure 1). The main differences involve (1) the collecting aperture and (2) the loss of light by absorption and reflection, and can be expressed as an intensity scaling factor. The calculation of this factor was as follows. For the *in vivo* situation, we assumed the general eye model of Le Grand and El Hage[15] and losses of light in the ocular media based on the mean data[16] given by Pokorny et al.

Ad 1. We used ray tracing to find the solid angle at the retina by which the photomultiplier ''sees'' the illuminated spot (the collecting aperture). In the *in vitro* setup, a column of blood behind a 0.8 mm cuvette wall replaced the retina. Due to the differences in optics (i.e., focal lengths), different magnifications occur: the collecting aperture *in vivo* proved to be larger than the one *in vitro;* the correction factor was 0.314.

Ad 2. In the *in vivo* situation, loss of light in the ocular media at 488 (excitation light) and 530 nm (fluorescent light, simplified) were calculated for the mean age of our subjects (21.8 years). The data given by Pokorny, Smith, and Lutze[16] are relative to the optical density at 700 nm. Estimating the absolute light loss at 700 nm to be 0.05, the total density was $D_{488} + D_{530} + D_{700} = 0.152 + 0.096 + 2 \times 0.05 = 0.348$, and the efficiency $10^{-0.348} = 0.449$. *In vitro*, only Fresnel losses due to different refractive indices (air$=1$, glass$=1.52$, Perspex $=1.49$ and blood$=1.35$) had to be taken into account, resulting in an efficiency of 0.772.

Multiply (1) and (2). To compare *in vivo* and *in vitro* intensities, the *in vivo* intensities had to be multiplied by $0.314 \times (0.772/0.449) = 0.54$. Individual differences in light loss and ocular dimensions limit the accuracy of this calculation to about 25%.

References

1. A. Wessing, *Fluoreszenzangiographie der Retina. Lehrbuch und Atlas*, pp. 11–16, Georg Thieme, Stuttgart (1968).
2. F. C. Delori, M. A. Castany, and R. H. Webb, ''Fluorescence characteristics of sodium fluorescein in plasma and whole blood,'' *Exp. Eye Res.* **27**, 417–425 (1978).
3. G. N. Lambrou, *Choroidal Plerometry. A Method for Evuation the Choroidal Blood Supply in Clinical Practice*, p. 85, Kugler, Amsterdam (1993).
4. P. R. van den Biesen, F. H. Jongsma, G. J. Tangelder, and D. W. Slaaf, ''Shear rate and hematocrit dependence of fluorescence from retinal vessels in fluorescein angiography,'' *Ann. Biomed. Eng.* **22**(5), 456–463 (1994).
5. J. R. Lakowitz, *Principles of Fluorescence Spectroscopy*, pp. 257–267, Plenum, New York (1983).
6. K. G. Romanchuk, ''Fluorescein, Physicochemical factors affecting its fluorescence,'' *Surv. Ophthalmol.* **26**(5), 269–283 (1982).
7. R. F. Brubaker, J. T. Penniston, D. A. Grotte, and S. Nagataki, ''Measurement of fluorescein binding in human plasma using fluorescence polarization,'' *Arch. Opthalmol.* **100**, 625–630 (1982).
8. D. van Norren and J. van de Kraats, ''Instrument note. Imaging retinal densitometry with a confocal scanning laser ophthalmoscope,'' *Vision Res.* **29**(12), 1825–1830 (1989).
9. International Commission of Non-Ionizing Radiation Protection, ''Revision of guidelines on limits of exposure to laser radiation of wavelengths between 400 nm and 1.4 μm,'' *Health Phys.* **79**(4), 431–440 (2000).
10. D. du Bois and E. F. du Bois, ''A formula to estimate the approximate surface area if height and weight be known,'' *Arch. Int. Med.* **17**, 863–871 (1916).
11. J. van Norel, P. R. van den Biesen, G. J. Groen, and D. van Norren, ''Hold up of dye in the arm during fluorescein angiography: A quantitative demonstration,'' *Am. J. Ophthalmol.* **129**(4), 551–552 (2000).
12. W. H. Press, B. P. Flannery, S. A. Teukolsky, and W. T. Vetterling, *Numerical Recipes in C*, pp. 521; 551–552, Cambridge University Press, Cambridge (1988).
13. H. Lund-Andersen, B. Krogsaa, M. la Cour, and J. Larsen, ''Quantitative vitreous fluorophotometry applying a mathematical model of the eye,'' *Invest. Ophthalmol. Vis. Sci.* **26**, 698–710 (1985).
14. W. F. Ganong, *Review of Medical Physiology*, 17th ed., pp. 518–520, Prentice–Hall International, London (1995).
15. Y. Le Grand and S. G. El Hage, *Physiological Optics*, pp. 57–69, Springer, Berlin (1980).
16. J. Pokorny, V. C. Smith, and M. Lutze, ''Aging of the human lens,'' *Appl. Opt.* **26**(8), 1437–1440 (1987).